COMPOSITION AND PHASE ANALYSIS ON GLAZED TILES OF SOUTHEAST ANATOLIA: PRODUCTION PROCESS IDENTIFICATION

Ömer Dabanlı*[1], Dursun Yıldız[2] and Murat Bayazit[3]

[1]Department of Conservation of Cultural Heritage, Faculty of Architecture and Design, Fatih Sultan Mehmet Vakif University, Istanbul, Turkey
[2]Diyarbakır Museum, Diyarbakır, Turkey
[3]Department of Ceramics, Faculty of Fine Arts, Batman University, Batman, Turkey

ABSTRACT

The analytical characterization of cultural heritage materials has a great importance in terms of gaining the scientific knowledge which provides guidance for conservation applications covering the re-integration and re-production processes needed in protection. In this study, the glazed tile samples of a 15th century monument located in southeast Anatolia are investigated and a comprehensive archaeometric data for restoration and conservation is created. XRF and EDX were used to reveal the chemical composition of tile bodies and particularly the glazes. SEM and petrography analyses were employed to examine the micro and macro structural features of the bodies, respectively. Samples were exposed to X-ray diffraction for characterization of the mineral/phase contents. Furthermore, thermogravimetric differential thermal analysis and Fourier transformed infrared spectrometry were the complementary methods. The mineralogical content of the samples suggested a firing temperature of ca 850-900ºC. The chemical composition of the tile fabrics indicated use of calcareous raw materials due to relatively high CaO content. It was deduced that the alkaline and lead oxides were the main components of the glazes, with low lead oxide (<5 wt.%) for the samples PS-2, PS-4, PS-5 and PS-6. It was also seen that the blue/green turquoise colors were obtained with copper, whereas blue itself was due to cobalt. Tin was occasionally detected in chemical composition of some glazed surfaces, and its presence was mostly attributed to the purpose of gaining opaqueness.

1. INTRODUCTION

The characterization of historical materials has a great importance in terms of protecting the cultural heritage. While the information obtained from the characterization studies provides guidance in terms of the conservation interventions to be applied to the material, it also yields a significant data basis regarding the re-integration and re-production that may be needed in some cases. As it is known, archaeometry is widely used as one of the significant research fields to investigate the historical and archaeological materials (Bianchin et al., 2009; Bayazit et al., 2014; Medeghini et al., 2016; Uzun et al., 2018; Zacharias et al. 2020; Liritzis et al., 2020;).

In the available literature, there are specific methods applied for ceramics and glazed tiles which are generally performed to obtain data concerning the chemical and mineralogical contents of the body and glazes (Ebaid and Ghaly, 2013; Bayazit et al., 2014; Fischer and Hsieh 2017; Bayazit, 2018; Panagopoulou et al., 2018; Simsek et al. 2019a, 2019b; Liritzis et al., 2020). For these kinds of purposes, spectroscopic and microscopic techniques step forward. The glaze layers on tiles could be investigated by scanning electron microscopy-energy dispersive X-ray spectrometry (SEM-EDX) in labs or by portable X-ray fluorescence (p-XRF) spectrometers both in labs and in-situ analyses, as mostly preferred (Fischer and Hsieh 2017; Messina et al., 2018; Simsek et al. 2019a, 2019b; Belfiore et. al., 2021). While the micro structural and micro chemical properties of the layers (body, slip and glaze) could be thoroughly examined by SEM-EDX, the opportunity of carrying out in-situ analyses with the non-destructive portable XRF devices gives a substantial advantage in terms of many aspects such as preventing time loss, chance for analysing all the spots that you can reach in the historic places, no need for sample preparation, and preservation of the original material.

A disadvantage for the portable device could be the detection limitation of some elements (e.g. some devices may not identify the elements with the atomic number under 11). Although the limitations may cause some problems in certain cases, the comprehensive works regarding the determination of colouring agents of glazed tiles showed that portable XRF is a very effective tool which gives a broad data range to be used in making conclusions and also comparisons with the previous literature (Fischer and Hsieh 2017; Simsek et al. 2019a, 2019b). In addition, X-ray diffraction (XRD) and petrography are the most used techniques for the tile bodies in order to reveal the mineralogical contents, while Fourier transformed infrared (FTIR) spectrometer and thermogravimetric – differential thermal analysis (TG-DTA) are the other methods preferred as the complementary ways to characterize the body composition (Bayazit et al., 2014; Bayazit, 2018).

In Parlı Safa Mosque, which is located in Diyarbakır, Southeast Anatolia (Fig. 1), the original glazed tile decorations had been implemented on both interior and exterior facades. While the tile ornaments were used for the minaret base on the exterior facade, they were utilized for cladding of the harim (main sanctuary space) walls of the mosque. The interior walls are covered with tiles up to 120 cm high from the floor. The tiles on the south, north and west walls have survived to the present day (partly preserving their originality), whereas the tiles on the eastern front have been destroyed. The glaze losses and some contaminants such as cement and/or gypsum could be observed on various walls of the mosque, and the missing tiles were occasionally represented by using oil paint on plaster applied on the walls (Baş, 2006; Gürsoy, 1993). Fig. 2 shows an overview for the tiles located near mihrab and the state of conservation of tiles can be observed in Table 1 (Baş, 2006; Gürsoy, 1993).

Two different compositions are generally observed on the walls of the harim. The first composition is the triangular and hexagonal composition on the north, east and southeast walls. The other composition for the tiles surrounding the interior wall is the geometric compositions formed by the intersection of the dodecagons on the western side of the south wall. The composition formed by the intersection of triangles, hexagons and dodecagons is surrounded by border tiles from the top and bottom. The composition of stylized flower and cloud motifs on border tiles are connected by simple branches (Yıldırım, 2001).
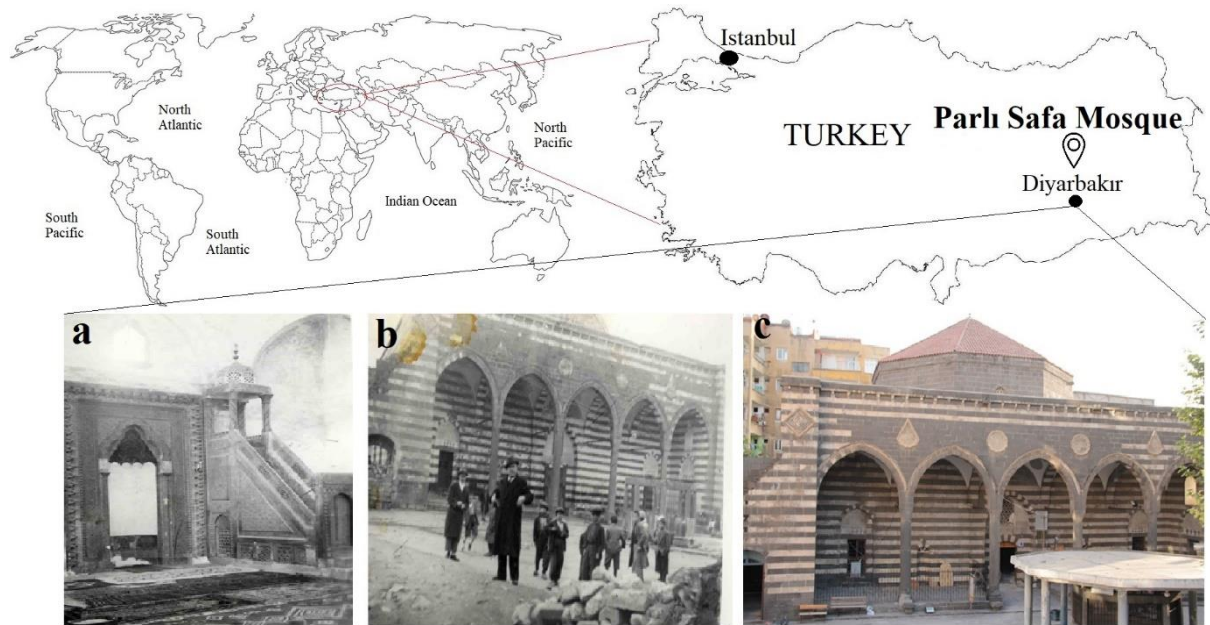
Figure 1. Location and views of the mosque sanctuary space (a) and, narthex (b) before 1955, (c) portico (VGM Archive).

Figure 2. (a) Glaze loss, (b) missing tiles occasionally represented by using oil paint, (c) contaminants (cement and/or gypsum), (d) overview of the tiles near mihrab (southern facade of the mosque).

The aim of this study is the identification of composition and phases of the glazed tiles used in Parlı Safa Mosque to clarify their production features. As far as is known, there are mainly three techniques applied in production of Diyarbakır tiles which are underglaze, coloured glaze and embossment (Baş, 2006; Demiriz, 2002). The use of coloured glaze technique could be only seen in Parlı Safa Mosque among the glazed tiles in Diyarbakır, and contours (a kind of barrier) are created with the help of brushes (for the tiles comprising multi-coloured glazes) in order to avoid the mixing of different colours on the surface of the tiles (Demiriz, 2002). These contours begin to swell during the firing process and generate a barrier between the colors, which hereby allows the craftsman/artist to use various coloured glazes on the same surface (Demiriz, 2002). It is known that coloured glaze technique has been used successfully until the emergence of the underglaze method and it has started to lose its effect during the 16th century (Baş, 2006; Demiriz, 2002). Considering the unique features of the tiles of Parlı Safa Mosque, a multi-analytical analysis procedure was applied for the representative samples in order to reveal the chemical and mineralogical contents which would lead to specify the production process through a comprehensive archaeometry approach.

Table 1: Deterioration levels of the tiles.

Wall	Description	Deterioration
North	Plaster was occasionally used on the surface (e.g. intersection areas of the windows), and the pseudo appearance of the tiles was provided with oil paint. Glaze loss on the tiles and some residuals referring to inappropriate repair/restoration material were observed. Original Oil Paint 	 Glaze loss Contaminants
South	A pseudo appearance of tiles (likewise the northern wall) was obtained by oil paint. On various areas of this facade, there are losses of glaze and component. The missing tile borders on windows' intersection points were completed with blue oil paint. In general, residues such as gypsum and cement were seen on the surfaces of the tile bodies.	 Profile view
East	The missing tiles were represented by oil paint on plaster. There are glaze and body losses. The tile borders (on window edges) were completed by blue oil paint. Gypsum and cement are observed on the surfaces.	 Gypsum/cement residues
West	Tile shapes were obtained with oil paint on plaster. While glaze losses were observed in the upper and lower borders, tile losses were seen under the silicone. Blue oil paint was used for completion of the tiles on the window edges. Cement and gypsum remain are seen on the tiles throughout the western wall. There are piece and glaze losses in the lower parts of the tiles.	 Gypsum/cement residues

2. EXPERIMENTAL STUDY

2.1. Materials

Being located in southeastern Anatolia, Diyarbakır has been one of the significant cities in the upper Tigris region. The name of the city has been mentioned as "Amidi" in Assyrian sources, "Amido" or "Amida" in Greek and Latin sources, and "Amid" in Arab sources. Since Diyarbakır is located at the intersection of trade routes, it has been an important city throughout the history. The city also undertook significant military duties, and the city walls that have
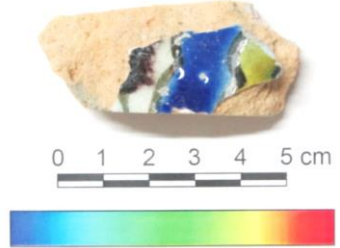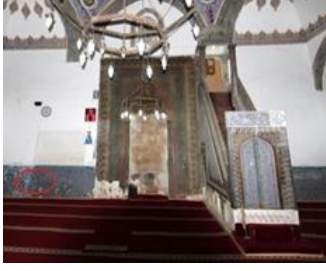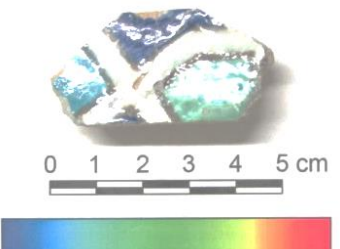
survived till today have made the city a strong settlement point. During the Ottoman period, Diyarbakır was an important center and served as a base for expedition troops Parlı Safa Mosque is located at the north-west of Diyarbakır city wall (in southeastern Anatolia) and has been defined by two different names in history: "Safa Mosque" and "İparlı Mosque" (Yediyıldız, 2008; Tuncer, 1996; Beysanoğlu, 1996).
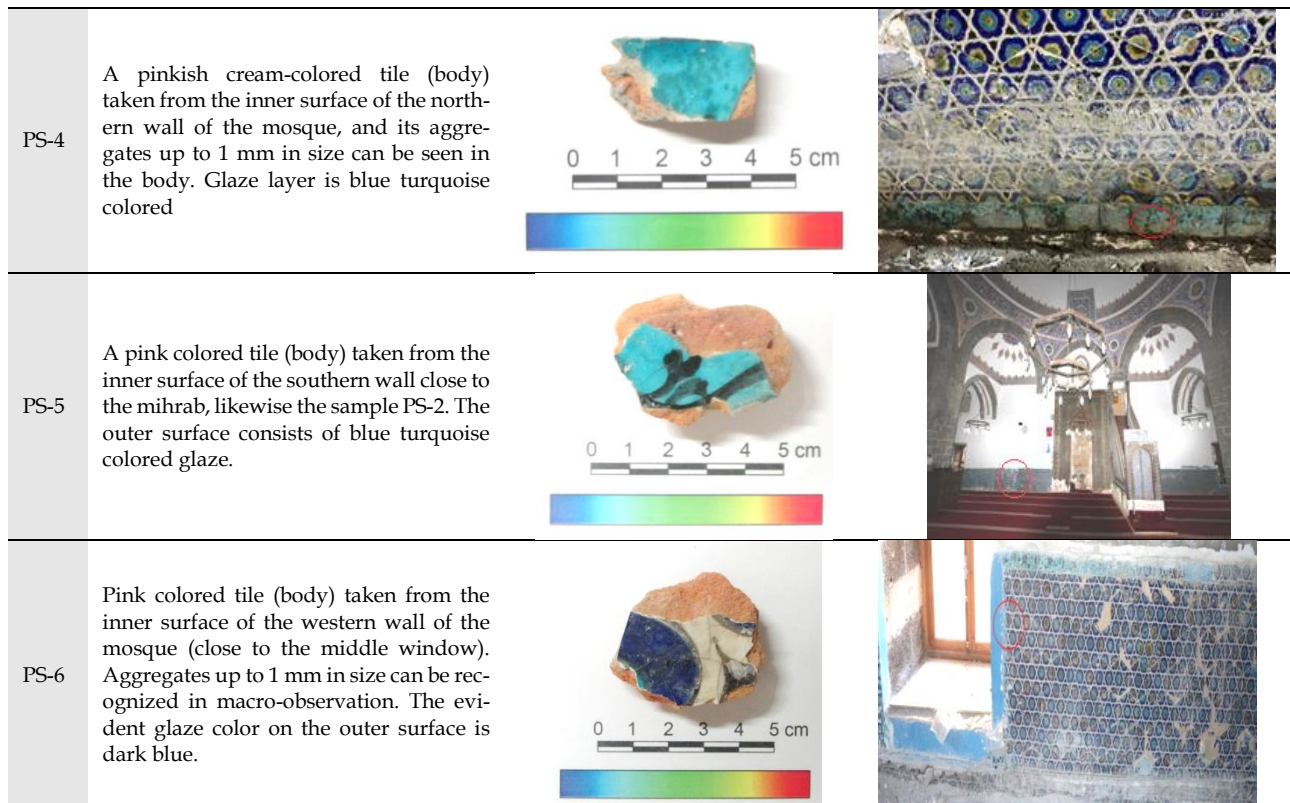
There are different arguments regarding the construction date of the mosque. Despite the absence of construction inscription, there is a restoration inscription on the entrance door of the mosque suggesting that it would have been built in Akkoyunids period (ca 1404-1515 AD). It is stated in the sources that the mosque was built by Uzun Hasan in the middle of the 15th century AD upon the order of Cüneyt (the son of Sheikh Ibrahim Safi) and was called "Cami'üs Safi" with respect to the sheikh, and then it has turned into "Camiü's Safa" in public ("cami" means "mosque" in Turkish). According to the inscription on the entrance gate, the construction was repaired by Hacı Hüseyin (son of Abdurrahman from Diyarbakır) in 1513 AD and this strengthens the possibility that the mosque was built by Uzun Hasan. The mosque has importance because of its architectural style, glazed tiles, stone decoration and ornamented minaret (Tuncer, 1996; Sözen, 1971).

There are six main types of glazed tiles used on the exterior and interior facades of the mosque. Taking into account all types, six tile samples representing the glazed tile repertoire of the mosque were selected (Table 2). While one sample belongs to an exterior facade (western side of the minaret), five samples are from various interior facades of the mosque (southern wall close to the mihrab, western wall and northern wall). At this stage, the representative samples were selected considering the paste structure and the colour diversity on the glazed surface so as to reflect the glazed tile repertoire of the mosque. The samples were initially cleaned with distilled water and photographed from both sides in order to document their original view. There was no additional surface treatment for the body and glaze layer of the samples other than cleaning with distilled water. Furthermore, powder samples were prepared in a porcelain mortar by grinding the body fragments obtained from the unglazed parts of the tiles and the powders were used in XRD, FTIR and TG-DTA analyses. Bulk samples were also arranged for the microscopic techniques (SEM-EDX and petrography). The glazed surfaces were investigated through SEM-EDX and portable XRF.

Table 2: Brief description and sampling locations of the tile samples.

Code	Description	General view	Sampling Location
PS-1	A pinkish cream-colored tile (body) taken from the outer surface in the area between the base and the cube section on the western side of the minaret. Aggregates up to 1 mm in size can be recognized in macro-observation. Glaze color on the outer surface is blue turquoise.		
PS-2	A buff/pinkish cream-colored tile (body) taken from the inner surface of the southern facade of the mosque (close to the mihrab). Aggregates up to 1 mm in size can be recognized in macro-observation. There are different colored glazes on the outer surface; blue, greenish yellow and dark brown. Black contours are also seen between the colors		
PS-3	A cream-colored tile (body) taken from the inner surface of the western wall of the mosque (close to the middle window). Aggregates up to 1 mm in size can be recognized in macro-observation. The light green, light blue and dark blue colors were separated with black contours.		

PS-4	A pinkish cream-colored tile (body) taken from the inner surface of the northern wall of the mosque, and its aggregates up to 1 mm in size can be seen in the body. Glaze layer is blue turquoise colored		
PS-5	A pink colored tile (body) taken from the inner surface of the southern wall close to the mihrab, likewise the sample PS-2. The outer surface consists of blue turquoise colored glaze.		
PS-6	Pink colored tile (body) taken from the inner surface of the western wall of the mosque (close to the middle window). Aggregates up to 1 mm in size can be recognized in macro-observation. The evident glaze color on the outer surface is dark blue.		

2.2. Methods

Considering the analytical techniques applied on glazed tiles, this study focuses on elucidating the production details of the tiles through the examination of the paste and especially the glazes in order to clarify for reproduction of the missing tiles to be used in restoration process of the mosque. For that purpose, SEM-EDX and portable XRF spectrometer were used to determine the chemical composition of the body and glaze. XRD and petrography were used to enlighten the mineralogical content of the samples, while TG-DTA and FT-IR spectrometer were used to examine the enthalpy changes and the characteristic spectra of the minerals, respectively. A Hitachi SU3500 scanning electron microscopy equipped with an Oxford EDX spectrometer was used to investigate the micro structural and micro chemical properties of the bodies and the coloured glaze layers. The analyses were carried out on fresh-fractured samples at various pressure (VP) mode of the SEM device (15 kW for acquisition). The working distance was approximately 10 mm. Elemental mapping was used on SEM images for some of the glazed surfaces and paste of the samples. EDX was employed on the selected areas of SEM images (with the scales changing in the range

of 50-1000μm) belonging to both the glazes and bodies. EDX data were in the form of elemental concentration, and they were transformed into oxides as wt. % which is conventionally used. The mineral/phase contents of the tile bodies were revealed by a Rigaku Miniflex-2 X-ray diffractometer using Cu-Kα with the working parameters of 30 kW, 15 mA. XRD analyses were carried out in the range of 0-60 2θ.

A portable XRF device of Olympus (Innov-X) was utilized for the colored glaze surfaces of sufficient size. Taking into account the dimensions of the tile samples (Table 2) and the size of colored sections (also the color transitions and the fine contours on some samples), portable XRF was employed for the areas which completely covered the scanning section of the device. Such application allowed making reliable measurements and let the portable device carry out the analyses with minimal errors (the device automatically stops the radiation emission and cancels the analysis, in case of incomplete closure of the sample holder). This technique, in addition to EDX, was used to enlighten the characteristics of the coloured glazes. The p-XRF analyses were carried out through "alloy mode" (scanning duration of 35 seconds) and "geochem mode" (scanning duration: 140 seconds) for the glazes and bodies. In the course of p-XRF characterization in "alloy mode", the samples were exposed to i[1]: Beam-

---

[1] Detectable elements: Ti, V, Cr, Mn, Fe, Co, Ni, Cu, Zn, Hf, Ta, W, Re, Pt, Au, Hg, Pb, Bi, Zr, Nb, Mo, Pd, Ag, Cd, Sn, Sb.

1 at 40 kV, ii[2]: Beam-2 at 13 kV and iii[3]: Beam-3 at 8 kV. In geochem[4] mode of p-XRF, the samples were exposed to i[5]: Beam-1 at 40 kV, ii[6]: Beam-2 at 10kV.

Petrographic investigation of the tile bodies was carried out using a LEICA Research Polarizan (DMLP) optical microscope which has top and bottom illumination. Images were taken from the thin sections (prepared from the tile bodies) with a Leica DFC280 digital camera (x25 magnification, single & double nicol). Petrography results were interpreted through the method of point counting together with the program of Leica Qwin digital imaging. In the course of petrographic investigation, the matrices of samples were firstly scanned through their thin sections, then the evident minerals and rock fragments were identified for each sample.

The bodies were additionally investigated by FTIR technique in which a Perkin Elmer 400 spectrometer was employed. The working range was 500-1800 cm^{-1}, as preferred in FTIR studies of ancient pottery (the finger print region). Tile bodies were finally characterized through a thermal analysis technique. For this purpose, the powder samples were investigated with a Shimadzu DTG-60H TG-DTA device. The working range was 25-1000°C at which the endothermic and exothermic reactions together with the weight loss values were determined. Heating rate was 10°C/min and the analyses were carried out in nitrogen atmosphere.

3. RESULTS AND DISCUSSION

3.1. Characterization of glaze layers

The initial step of the study was to reveal the chemical composition of the glaze layers on the tile surfaces. Afterwards, the paste structures under the glaze layers were characterized to reach the knowledge of the raw materials used for production. In order to draw more reliable conclusions, EDX results were simultaneously assessed with the data obtained through the portable XRF applied on glazed surfaces of sufficient size. The elemental concentrations of the glazed surfaces and bodies characterized by EDX (as oxide forms) (Table 3) and p-XRF (using alloy and geochem modes) are listed in Table 4.

Table 3. EDX results (Oxide wt. %) of the samples (glaze and body).

Sample	Na$_2$O	MgO	Al$_2$O$_3$	SiO$_2$	CaO	PbO	K$_2$O	CuO	SnO$_2$	FeO	MnO	CoO	SO$_3$	P$_2$O$_5$	TiO$_2$	Cr$_2$O$_3$
PS-1																
Blue turquoise glaze	8.38	2.55	2.33	47.56	5.06	19.73	2.25	5.74	5.64	0.75	-	-	-	-	-	-
	7.82	2.49	2.47	47.64	5.56	20.09	2.35	5.48	5.34	0.77	-	-	-	-	-	-
Body	2.15	6.76	8.92	58.08	10.92	-	3.06	-	-	7.57	-	-	1.38	0.55	0.61	-
PS-2																
White glaze	8.36	5.42	2.04	74.27	4.19	-	3.30	0.84	0.57	1.01	-	-	-	-	-	-
Dark brown glaze	9.71	3.72	-	66.10	5.68	2.89	2.99	1.06		1.19	4.41	-	-	-	-	-
Blue glaze	10.68	4.04	1.51	71.75	5.73	1.55	3.17	-	-	1.05	-	0.53	-	-	-	-
Interlayer	17.07	3.93	1.97	67.93	5.45	-	2.64	-	-	0.39	-	-	-	-	-	-
Body	2.39	3.24	6.93	71.21	7.62		2.86			3.04	-		2.35		0.36	-
PS-3																
Light blue glaze	8.86	1.89	1.96	43.93	4.54	16.56	1.28	13.36	7.16	0.46	-	-	-	-	-	-
Light green glaze	2.11	-	1.32	37.16	1.79	42.42	1.40	5.23	7.26	1.31	-	-	-	-	-	-
Body	2.00	5.93	4.64	59.96	13.20	-	1.97	-	-	3.69	-	-	8.13	-	-	-
PS-4																
Blue turquoise glaze	13.78	-	-	64.48	4.94	1.64	1.95	12.80	-	0.41	-	-	-	-	-	-
Body	3.66	3.42	2.42	48.76	27.77	-	1.95	1.23	-	2.44	-	-	6.45	-	-	1.44
PS-5																
Blue turquoise glaze	6.35	5.27	2.51	64.13	8.55	2.67	1.90	2.34	-	0.68	-	-	2.64	1.37	-	1.19
Body	3.96	6.81	8.23	62.26	8.93	-	2.27	-	-	5.01	-	-	0.84	-	0.40	-
PS-6																
Blue glaze	1.41	25.49	1.41	58.98	6.32	-	1.60	-	-	1.17	-	0.88	2.19	-	-	-
Body	3.41	4.10	16.95	58.61	7.14	-	3.87	-	-	3.28	-	-	1.60	-	0.72	-

(-) : not detected or under the detection limit.

---

[2] Detectable elements: Mg, Al, Si, P, S, Mo, Sn, Ti, V, Cr, Mn, Fe, Co, Ni, Cu, Zn.

[3] Detectable elements: Mg, Al, Si, P, S, Mo, Sn, Ti, V, Cr, Mn, Fe.

[4] Please note that Na was out of the detection limits

[5] Primary detectable elements: V, Cr, Fe, Co, Ni, Cu, Zn, Pt, W, Hg, As, Se, Au, Br, Pb, Bi, Rb, U, Sr, Y, Zr, Th, Nb, Mo, Ag, Cd, Sn, Sb, Ti, Mn.

[6] Primary detectable elements: Mg, Al, Si, P, S, K, Ca, Ti, Mn.

The amounts (wt.%) of CuO (5.48-5.74), SnO₂ (5.34-5.64), PbO (19.73-20.09), Na₂O (7.82-8.38) and K₂O (2.25-2.35) identified on blue turquoise glaze of PS-1 (Table 3) are evaluated with the p-XRF results which revealed the existence of Cu, Sn and Pb in the glaze (Table 4). It was deduced from the whole data that copper and tin were effective information of the blue turquoise color. The results showed that the glaze comprised alkaline and was rich in lead.

EDX data (Table 3) obtained from three different colored glaze layers on the sample PS-2 (white, dark brown and blue) suggested that an alkali glaze containing low lead was used. Manganese was obviously detected by p-XRF on dark brown, while Co and Cu were seen on blue coloration (Table 4). The black contour between the colors was found to be achieved mostly with manganese (3.46 wt.% in p-XRF). Although it was expected that the presence of copper (detected by the EDX) on white area would cause a change in color, this content is likely to come from other colored glazes on the tile surface. Considering the small size of the tiles, close color transitions on the samples' surface and the focus range of the portable device, it would be possible to encounter such values in the course of analysis applications. The white area on the tile was expected to contain tin for the opacity, but its low amount suggested that such appearance would be related more likely to the white slip layer beneath the glaze (Fig. 3b for the interlayer). It was concluded from the chemical composition of the glazes on this sample that the blue color was brought by cobalt, while the dark brown was due to manganese. The high amount of Na₂O (17.07 wt.%) detected in EDX analysis carried out on the intersection point of the glaze and interlayer confirmed the alkali character of the glaze (Fig. 3).

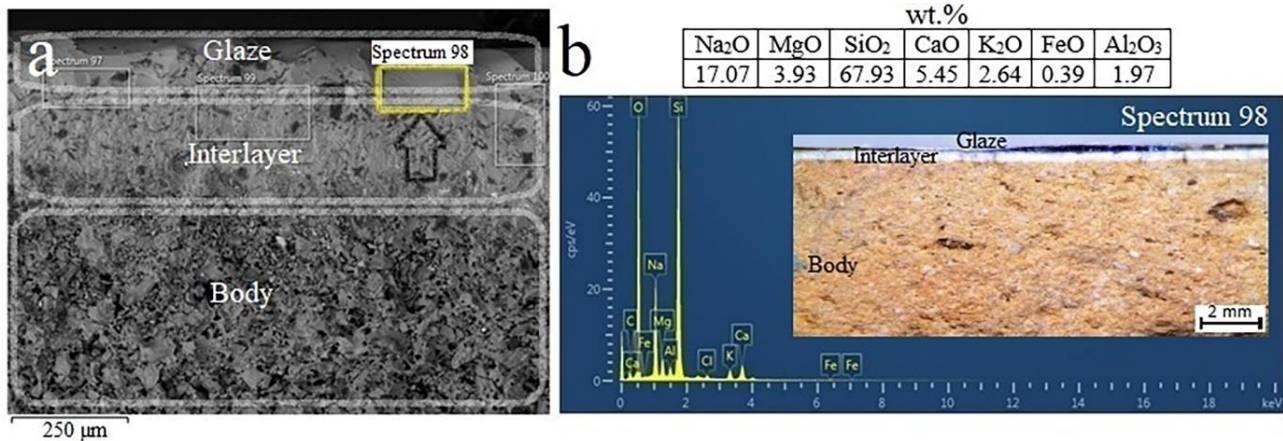|			wt.%			
Na₂O	MgO	SiO₂	CaO	K₂O	FeO	Al₂O₃
17.07	3.93	67.93	5.45	2.64	0.39	1.97

Figure 3. SEM image of the sample PS-2 (a) interlayer between the body and glaze, (b) EDX results of the selected area.

According to the chemical composition of sample PS-3 (Table 3 and Table 4), it was seen that the glaze was a lead-alkali one which included copper (bringing both the light blue and green turquoise colors) and cobalt (giving the dark blue color). Alkaline oxides and lead content in the glaze composition are predicted to be the key factors in obtaining different colors on the same surface with copper. While the light blue color seems to be derived by high alkali content, it is deduced that green color was obtained with the increase in lead content (EDX; PbO amount from 16.56 wt.% to 42.42 wt.%, p-XRF alloy mode; Pb amount from 36.26 wt.% to 64.94 wt.%, p-XRF geochem mode; Pb amount from 10.45 wt.% to 28.41 wt.%) (Yastı, 2011). This assumption was additionally proved by the chemical composition of the dark blue glaze characterized solely by p-XRF in the study. The data obtained by p-XRF for light blue, light green and dark blue glazes suggested that increase in the amount of lead brought the lighter blue and afterwards it might turn into green, depending on the presence of copper and tin, as well (Table 4). Tin seems to be effective in formation of such colors for the sample PS-3 (excluding dark blue), but this content may also have been used for glaze opacity (Mason and Tite, 1997). Considering the close concentrations of tin oxide detected by EDX (7.16 and 7.26 wt.%, respectively for the light blue and light green) and the ratio of PbO/SiO₂ (0,38 and 1,14 wt. %, respectively) (Table 3), it could be deduced from the data that, with a relatively low lead content in the first case, cassiterite (SnO₂) would have crystallized and rendered opaque the colour developed by the colouring element (copper for the light blue), and in the second case; the ratio of PbO/SiO₂ seems sufficient high for the development and persistence of the crystalline phase of PbSnO₃ that has a yellow colour which would have combined with the cooper and brought the light green color (Kühn, 1968; Tite et al., 2008).

Table 4. Elements identified by p-XRF (using alloy and geochem modes) and EDX (wt.%).

PS-1		Al	Si	Ca	Pb	Cu	Sn	Fe	Mn	Co	Cr	As	Bi	S	Ni
Blue turquoise glaze	alloy	1.37	41.6	-	41.39	3.02	11.61	0.70	-	-	-	-	-	-	-
	geochem	1.44	26.24	7.30	19.84	2.18	6.87	0.60	0.01	-	-	0.25	-	10.49	-
	EDX	1.24	22.23	3.62	18.32	4.58	4.45	0.58	-	-	-	-	-	-	-
Body	alloy	12.01	73.21	-	0.99	-	0.43	10.17	0.25	-	-	-	-	1.53	-
	geochem	3.99	25.27	3.64	0.09	0.003	-	1.50	0.02	-	0.01	-	0.001	0.56	-
	EDX	4.72	27.15	7.81	-	-	-	5.89	-	-	-	-	-	0.55	-
PS-2															
White glaze	alloy	2.39	78.37	-	10.2	0.46	-	4.2	2.34	-	0.64	-	-	-	-
	geochem						Not Applied								
	EDX	1.08	34.72	2.99	-	0.67	0.45	0.78	-	-	-	-	-	-	-
Dark brown glaze	alloy	2.46	52.01	-	18.66	1.02	-	6.12	14.42	-	1.99	-	-	-	-
	geochem						Not Applied								
	EDX	-	30.90	4.06	2.69	0.85	-	0.92	3.42	-	-	-	-	-	-
Blue glaze	alloy	2.98	77.6	-	5.91	0.46	-	4.46	0.47	2.10	-	2.25	2.10	-	0.56
	geochem	0.80	35.35	3.63	1.23	0.07	0.01	0.89	0.09	0.86	0.01	0.37	0.10	1.53	0.09
	EDX	0.80	33.54	4.09	1.44	-	-	0.82	-	0.42	-	-	-	-	-
Black contour	alloy	3.79	68.52	-	5.68	0.27	-	7.45	3.46	-	10.10	-	-	-	-
	geochem						Not Applied								
	EDX						Not Applied								
Body	alloy	14.62	75.62	-	0.38	-	-	6.51	-	-	-	-	-	-	-
	geochem	4.45	26.32	3.47	0.05	0.005	0.004	1.41	0.02	-	0.008	-	-	0.18	0.003
	EDX	3.67	33.29	5.45	-	-	-	2.36	-	-	-	-	-	0.94	-
PS-3															
Light blue glaze	alloy	-	46.29	-	36.26	6.65	7.77	0.98	-	-	-	-	-	-	-
	geochem	1.53*	46.00*	5.92*	10.45	3.10	3.05	-	-	-	-	0.31	-	6.81	-
	EDX	1.04	20.54	3.24	15.37	10.68	5.64	0.36	-	-	-	-	-	-	-
Light green glaze	alloy	-	27.71	-	64.94	2.43	2.24	1.83	-	-	-	-	-	-	-
	geochem	-	38.97*	-	28.41	1.75	1.50	1.69*	-	-	-	1.24	-	16.34	-
	EDX	0.70	17.37	1.28	39.38	4.18	5.71	1.02	-	-	-	-	-	-	-
Dark blue glaze	alloy	4.33	67.00	-	14.34	1.54	-	4.02	-	2.36	-	2.43	2.73	-	0.58
	geochem	3.13*	74.31*	4.05*	1.19	-	-	1.24*	-	1.02	-	0.36	0.10	1.32	0.10
	EDX						Not Applied								
Black contour	alloy	3.85	46.52	-	37.87	1.68	1.45	3.11	1.11	-	0.99	2.46	-	-	-
	geochem						Not applied								
	EDX						Not applied								
Body	alloy	8.73	76.75	-	1.94	-	-	12.14	-	-	-	-	-	-	-
	geochem	2.64	28.57	4.96	0.17	0.01	0.002	2.05	0.03	-	0.009	-	-	0.63	0.006
	EDX	2.45	28.03	9.43	-	-	-	2.87	-	-	-	-	-	-	-
PS-4															
Blue turquoise glaze	alloy	-	69.13	-	15.11	13.29	-	1.86	-	-	-	-	-	-	-
	geochem	0.20	30.65	4.18	1.02	2.01	0.005	0.41	0.037	-	0.025	0.03	0.001	0.96	-
	EDX	-	30.14	3.53	1.52	10.23	-	0.32	-	-	-	-	-	-	-
Body	alloy	8.72	78.31	-	0.81	-	-	10.54	0.44	-	-	-	-	-	-
	geochem	3.71	37.82	3.56	0.06	0.005	0.002	1.62	0.08	-	0.009	-	-	0.21	0.007
	EDX	1.28	22.79	19.84	-	0.98	-	1.89	-	-	0.99	-	-	2.58	-
PS-5															
Blue turquoise glaze	alloy	-	47.80	-	35.95	13.94	-	1.76	-	-	-	-	-	-	-
	geochem	0.35	14.88	5.14	2.19	2.00	-	0.38	0.01	-	-	0.04	-	2.00	-
	EDX	1.33	39.98	6.11	2.47	1.87	-	0.53	-	-	0.81	-	-	1.06	-
Body	alloy	9.71	79.20	-	0.68	-	-	9.36	0.59	-	-	-	-	0.43	-
	geochem	3.24	30.27	4.73	0.09	0.006	-	1.72	0.07	-	0.01	-	-	1.71	-
	EDX	4.36	29.10	6.39	-	-	-	3.90	-	-	-	-	-	0.34	-
PS-6															
Blue glaze	alloy	2.38	70.27	-	4.02	0.51	0.87	4.91	0.35	3.29	-	5.08	5.82	-	1.03
	geochem	0.82	29.35	3.00	0.18	0.05	0.03	0.71	0.02	1.19	0.01	0.39	0.13	1.23	0.12
	EDX	0.75	27.57	4.52	-	-	-	0.91	-	0.69	-	-	-	0.88	-
Body	alloy	15.24	68.24	-	0.21	-	-	6.88	-	-	-	-	-	6.94	-
	geochem	5.44	29.29	3.86	0.02	0.004	0.001	1.13	0.01	-	0.004	0.0006	-	0.29	0.003
	EDX	8.97	27.40	5.10	-	-	-	2.55	-	-	-	-	-	0.64	-

* Identified in the oxide form (i.e. Al₂O₃, SiO₂, CaO, Fe₂O₃). (-): not detected or under the detection limits.

EDX investigation of the blue turquoise glaze of the sample PS-4 carried out on different scaled SEM images showed that the glaze used in the sample was an alkali one containing low amount of lead (Table 3). The high alkali content on the glaze surface and the low amount of lead indicated that the blue (turquoise)

color on the sample surface was supplied with copper which was also detected through p-XRF (Table 4).

The chemical composition identified for the turquoise glaze layer of the sample PS-5 indicated that the glaze mostly included alkaline oxides rather than

lead (Fig. 4) and that the blue turquoise glaze was obtained with copper ions. For the sample PS-6 (Table 3 and Table 4), both the EDX and p-XRF analyses applied on blue glaze revealed the presence of cobalt which was detected as 0.88 wt.% (alloy mode) and 3.29-1.19 wt.% (geochem mode). Copper, tin and lead were the other elements identified by p-XRF for the blue glaze of PS-6. Such results showed that the blue color was brought by cobalt, while copper and tin were also thought to be effective in formation of the color. The low amount of lead identified for the glaze layer suggested a low lead-alkali glaze.

Scatter plots were additionally prepared in order to compare the chemical compositions of the glazes in general. Al vs. Si amounts and Al/Si vs. Ca/Si ratios identified through the portable XRF (in geochem mode) for the blue, turquoise and green colored glazes (also the white one) brought a convenient knowledge regarding the elemental composition of the glazes (Fig. 5). It could be seen from the scatter plots that Si content is relatively higher in dark blue glazes (Fig. 5a), whereas Ca/Si ratio is higher in light blue and blue turquoise glazes (Fig. 5b). It was observed that the dark and light blue glazes show an evident discrepancy, as expected considering the distribution area. Additionally, the fluctuation in amount of aluminum indicated use of different clay additives in the glaze mixtures. Finally, it was deduced that the amounts and ratios of the elements (Al, Si, Ca) evidently differentiate the dark and light blue glazes on the same surface of sample PS-3 (Fig. 5).
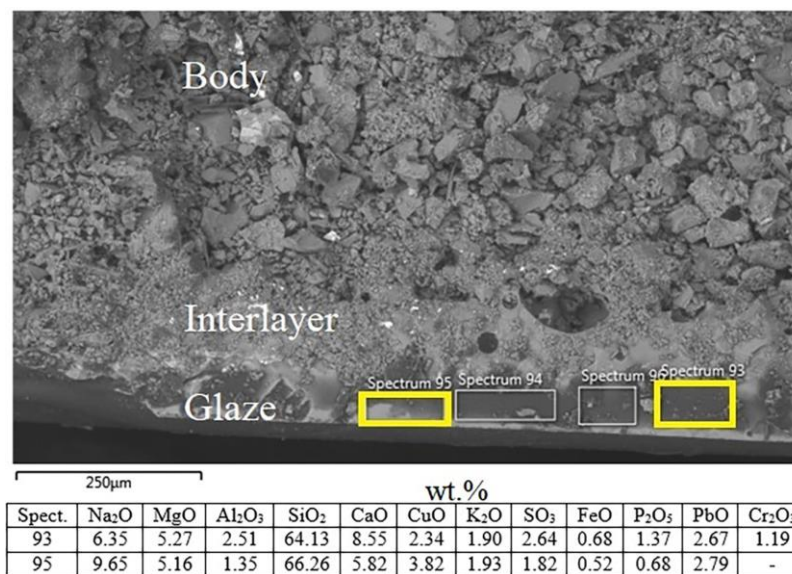

Spect.	Na₂O	MgO	Al₂O₃	SiO₂	CaO	CuO	K₂O	SO₃	FeO	P₂O₅	PbO	Cr₂O₃
93	6.35	5.27	2.51	64.13	8.55	2.34	1.90	2.64	0.68	1.37	2.67	1.19
95	9.65	5.16	1.35	66.26	5.82	3.82	1.93	1.82	0.52	0.68	2.79	-

Figure 4. SEM image of the sample PS-5 (turquoise glaze, interlayer and body), and EDX results of the selected areas.
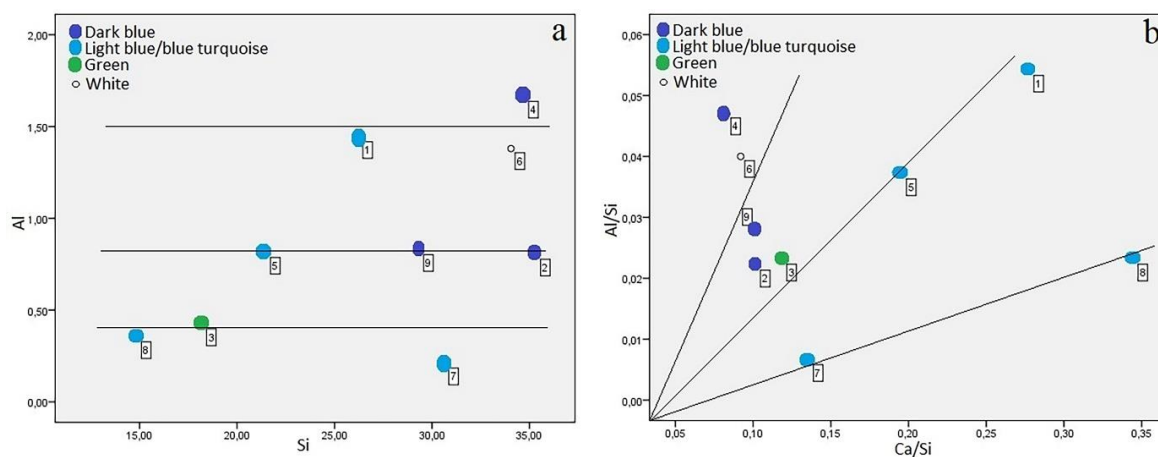

Figure 5. Scatter plots7 of (a) Al vs. Si amounts and (b) Al/Si vs. Ca/Si ratios identified by portable XRF (wt.%, in geochem mode) for 1. blue turquoise (PS-1), 2. dark blue (PS-2), 3. green (PS-3), 4. dark blue (PS-3), 5. light blue (PS-3), 6. white (PS-3), 7. blue turquoise (PS-4), 8. blue turquoise (PS-5), 9. dark blue (PS-6) glazes.

---

7 Lines are subsequently drawn as a guide for assessing the results.

A special attention was paid on cobalt which was thought to be responsible for the dark blue colored glazes on the samples PS-2, PS-3 and PS-6 (Table 2). For that purpose, the ratios of Co/Cu, Co/Ni, Co/Mn, Bi/Co, and also Sn/Pb (identified on dark blue colored glazes by p-XRF, in geochem mode) were compared with some of the representative results (Simsek et al., 2019a, 2019b; Fischer and Hsieh, 2017) obtained for the blue glaze/decors of tile/porcelain samples using portable XRF, as applied in the present research (Table 5). The data distribution areas in Fig. 6 a-b suggested that Parlı Safa tiles (PS-2, PS-3 and PS-6) generally differ from the other tile samples of Edirne mosques (Şah Melek Paşa/1429, Muradiye/1435–1436, Üç Şerefeli/1410–1447, and Selimiye/1569–1575) and Iznik production, and from the blue-white porcelain samples (Indonesia and Philippines) (Simsek et al., 2019a, 2019b; Fischer and Hsieh, 2017). It was seen that these three samples of Parlı Safa Mosque were clearly set apart from the others considering especially the ratio of Co/Ni (blue-white porcelain from Banten-Indonesia could be excluded since it is close to Parlı Safa tiles; Co/Ni: 8.44, Table 5 and Fig. 6a). Co/Mn ratio, too, shows a distinction between the samples of Parlı Safa Mosque and others, but this time PS-2 seems to be closer to the tiles of Edirne mosques and Iznik. It was additionally seen that the Co/Cu ratio is relatively higher for the samples of PS-2 and PS-6 in comparison with that of PS-3, which might be attributed to use of at least two different cobalt ores. Considering the presence of cobalt (identified on dark blue glazes) together with some of the decisive elements (e.g. Ni, Fe, As, Mn, Cu) (Table 4), which would be directive in determination of the cobalt type, it was deduced that the correlation among such elements relatively match with the European cobalt (mixture of Co-As-Ni-Fe) rather than the Asian (Co, Fe, Mn, no As) or Persian (Co, high amount of Fe, As, no Cu, Ni, Zn) (Simsek et al., 2019a, 2019b). This prediction was also approved by the simultaneous presence of nickel with arsenic and cobalt on the dark blue glazes.

Table 5. Comparison of Co/Cu, Co/Ni, Co/Mn, Bi/Co and Sn/Pb ratios (identified on blue glazes by p-XRF, in geochem mode) with the selected literature focusing on blue glaze/decors of ceramics/tiles using portable XRF*.

No	Sample/Location	Analyzed spot	Co/Cu	Co/Ni	Co/Mn	Bi/Co	Sn/Pb
1	PS-2 (present study)	Blue glaze	11,67	9,18	9,45	0,12	0,007
2	PS-3 (present study)	Blue glaze	4,21	9,31	35,33	0,1	0,012
3	PS-6 (present study)	Blue glaze	22,45	9,23	40,09	0,11	0,18
4	[a] Blue-white porcelain from Banten (Indonesia) BT-01	Blue spot on blue-and-white porcelain	16,71	3,12	0,18	n.a.	not defined
5	[a] Blue-white porcelain from Banten (Indonesia) BT-02	Blue spot on blue-and-white porcelain	66,52	8,44	0,15	n.a.	not defined
6	[a]Blue-white porcelain from Guthe (Visayas, Philippines) GU-01	Blue spot on blue-and-white porcelain	1,29	2,43	0,05	n.a.	not defined
7	[a]Blue-white porcelain from Guthe (Visayas, Philippines) GU-02	Blue spot on blue-and-white porcelain	6,89	1,09	0,19	n.a.	not defined
8	[b] Edirne, Selimiye Mosque	Blue decor	not defined	n.a.	0,4	4,5-6	0,081 (in average)
9	[b] Edirne, Selimiye Mosque	Blue decor	0,1-0,3	3,0-4,0	1,5-3,0	1,5-3,0	
10	[b] Edirne, Muradiye Mosque	Blue decor	0,4	n.a.	0,65	0,2-0,6	0,234 (in average)
11	[b] Edirne, Muradiye Mosque	Blue decor	0,01-0,004	notdefined	5	6,5	
12	[b] Edirne, Şah Melek Paşa Mosque	Blue decor	0,7	2,1	1,0-8,0	2,1	0,305 (in average)
13	[b]Edirne, Şah Melek Paşa Mosque	Blue decor	0,6	1,9	0,1-0,9	1,9	
14	[b]Edirne, Üç Şerefeli Mosque	Blue decor	0,01	0,8	n.a.	7,5	~ 0
15	[b]Edirne, Üç Şerefeli Mosque	Blue decor	0,1	0,8	n.a.	0,8	(in average)
16	[c]Iznik tile (B7-10)	Blue spot on glazed tile	0,28	1,73	0,72	3,26	0,002
17	[c]Iznik tile (B7-12)	Blue spot on glazed tile	0,09	1,53	n.a	8,84	0,006
18	[c]Iznik tile (B7-17)	Blue spot on glazed tile	1,28	2,18	8,25	0,95	0,007
19	[c]Iznik tile (B7-15)	Blue spot on glazed tile	0,91	1,59	4,42	2,52	0,018
20	[c]Iznik tile (B8-2)	Blue spot on glazed tile	0,78	2,69	4,46	1,07	0,008

* Only representative results are given here. The whole data associated with the articles can be obtained from the relevant references and their supplementary files given in online versions ([a] Fischer and Hsieh, 2017; [b] Simsek et al., 2019a; [c] Simsek et al., 2019b).

Arsenic changes from 0.03 wt.% to 0.25 wt.% for the blue turquoise, whereas it is higher and changes in a very narrow range (0.36-0.39 wt.%) for the dark blue glaze (Table 4). An exception was the light blue glaze of PS-3 which possesses 0.31 wt.% As, but no traces of Co, Ni or Bi. Identification of arsenic on blue glazes (regardless of light, dark or turquoise blue) and bismuth (only for the dark blue glazes; PS-2, PS-3 and PS-6, excluding its ignorable amount on blue turquoise glaze of PS-4: 0.001 wt.%) might suggest that such ingredients in tiles could be associated with the

hypothesis of Porter regarding the utilization of European cobalt, and also with Constantinescu's mention referring to a compositional change in the recipe of blue glazes after 1520 which claims a decrease in nickel and iron quantities together with the emergence of bismuth and arsenic (Constantinescu et al., 2014). On the other hand, in terms of Bi/Co ratios (Fig. 6b), it was also observed that PS-2, PS-3 and PS-6 are close to some characteristic samples of Muradiye Mosque (Edirne, 15th century), Üç Şerefeli Mosque (Edirne, 15th century) and Iznik (16th-17th century) (Simsek et al., 2019a, 2019b).
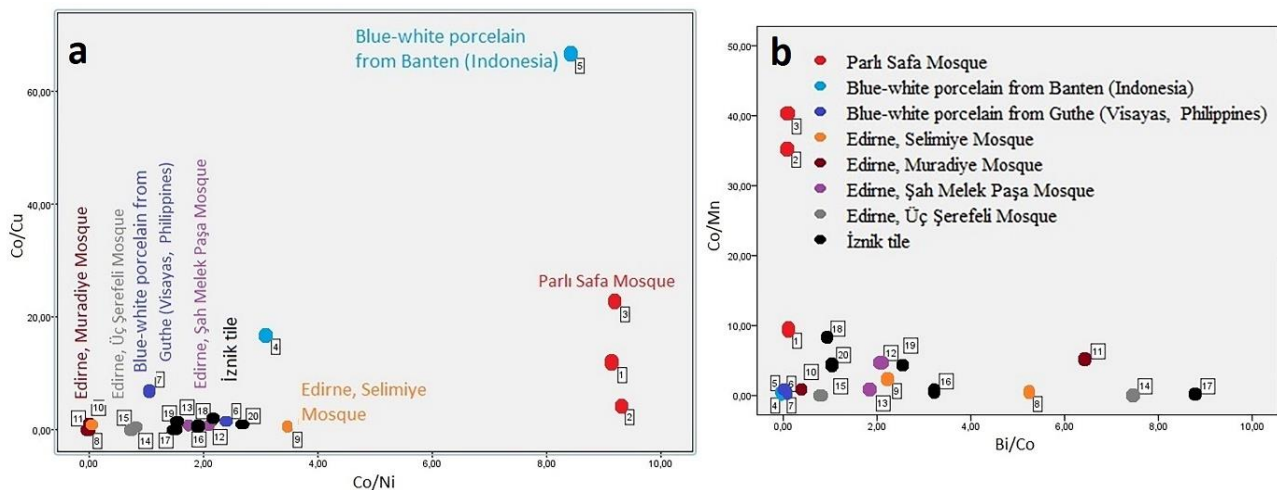
Figure 6. Scatter plots showing the weight ratios of (a) Co/Cu vs. Co/Ni and (b) Co/Mn vs. Bi/Co.

Finally, sulphur and calcium were detected on blue colored glazes in the range of 0.96-10.49 wt.% and 2.89-7.30 wt. %, respectively (Table 4). The presence of sulphur in such amounts with calcium suggested possible use or addition of lapis lazuli which was formerly documented since Ptolemaic Dynasty (13th-15th centuries) (Colomban, 2003; Caggiani et al., 2013).

The amounts Fe, Cr and Mn detected on the black lines of two samples (detected by p-XRF in alloy mode for PS-2 and PS-3) indicated that these contours between the colored glazes have most likely been achieved by using particularly manganese (3.46 wt.% for PS-2 and 1.11 wt.% for PS-3), and would be also associated with iron (7.45 wt.% for PS-2 and 3.11 wt.% for PS-3) and chromium (10.1 wt.% for PS-2 and 0.99 wt.% for PS-3). The ratio of Fe/Mn (2.15 for PS-2 and 2.80 for PS-3) and the scatter plots prepared through the ratios of Fe/Si vs. Mn/Si and Fe/Si vs. Cr/Si identified on the black contours (Fig. 7) make the tiles closer to the samples of Muradiye Mosque (1435-1436) and Şah Melek Paşa Mosque (1429) of Edirne (Simsek et al., 2019a). Although Fe/Mn ratios of Parlı Safa tiles are far away from Iznik samples belonging to the 16th and 17th centuries (Simsek et al., 2019b), the evident identification of chromium in PS-2 could be related to use of this element for the black line in Iznik

samples of 16th century (Colomban, et al., 2004). As the polychrome tiles of Muradiye Mosque showed the clear presence of manganese and absence of chromium (Simsek et al., 2019a), Parlı Safa samples (PS-2, PS-3) differ from these tiles particularly in terms of chromium existence. Considering the whole analytical data, it could be deduced that the black contours on such samples have presumably been implemented by using different combinations of Fe, Mn and Cr.

In the present study, the glaze types are found as the lead-alkali and low lead-alkali. This result suggested that the tiles would have been produced with two types of glazes. In principle, use of lead or lead-alkali glazes seems more advantageous than the alkali ones (including 15-20 wt.% alkali and no lead) since the alkali components and/or the additives such as natron or plant ash in the glaze are soluble in water and consequently such glaze should be initially fritted (preferably with silica), excluding the Chinese alkali glazes possessing saltpeter (Tite et al., 1998; Wood et al., 1989). Another advantage of the glazes comprising lead is that they are not prone to cause any defects on glaze and/or body (e.g. crazing, shattering, shivering), considering the thermal expansion coefficients (Tite et al., 1998). For the present case of Parlı Safa Mosque, the chemical content of the glazes

suggested that the lead content would have been de-liberately added so as to take the advantage of such type of glazes. Considering the directive work of Hurst and Freestone (1996) focusing on differentia-tion of whether the lead was solely used or it was mixed with silica (Hurst and Freestone, 1996), it was deduced from the chemical composition data that a lead-silica mixture would likely have been added to the glazes of the tiles, since it was seen that when the lead and colorants were extracted from the glaze and the chemical composition was re-calculated by nor-malizing to 100 wt.%, the new data did not match with that of the tile body.
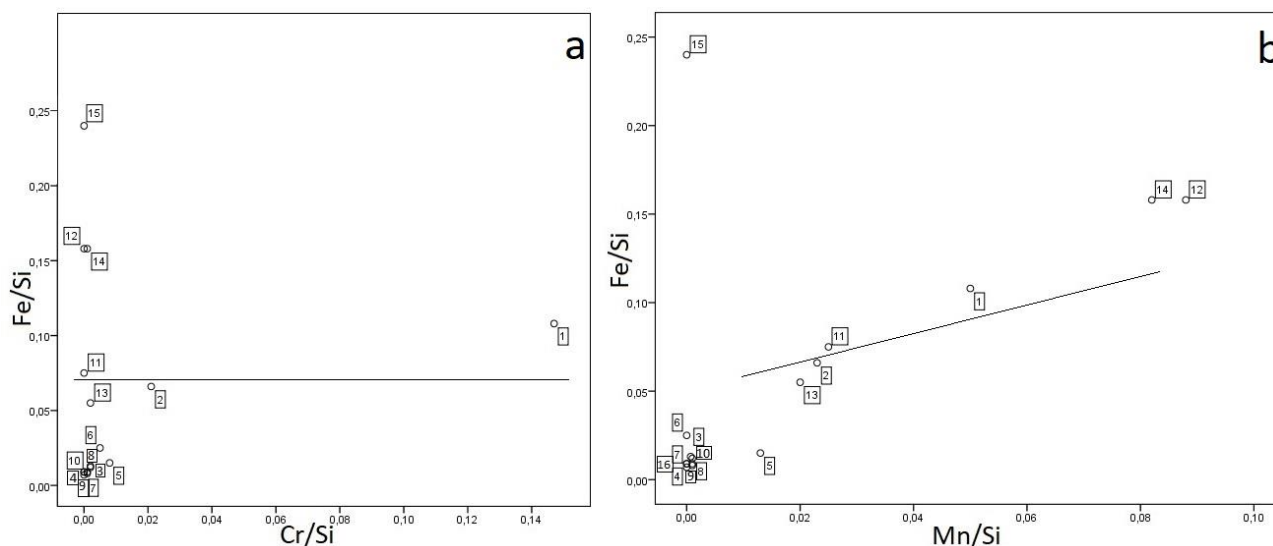
Figure 7. Scatter plots of (a) Fe/Si vs. Cr/Si and (b) Fe/Si vs. Mn/Si ratios identified by p-XRF (wt.%, in alloy mode). 1: PS-2, 2: PS-3, 3-10: Selimiye, 11-12: Muradiye, 13-14: Şah Melek, 15-16: Üç Şerefeli Mosques (Simsek et al., 2019a).

Tin was clearly detected for the glaze layers of the samples PS-1, PS-2, PS-3 and PS-6 (Table 3 and Table 4). The presence of tin in such samples therefore might be attributed to its use as an opacifier which, in a way, is consistent with the use of this element for the purpose of gaining opacity in history (Mason and Tite, 1997). It would be assumed from our data that such application seems to have been used in the 15th-16th century AD in southeast Anatolia, but only in case of a local production. The available literature suggests that in addition to the other manufacture centers like Iznik, Kütahya and İstanbul, traditional glazed tiles have also been locally produced in Diyar-bakır, which was approved by the presence of ce-ramic kiln residues, but the occasional use of Iznik tiles on some of the mosques (e.g. Behram Paşa Mosque, Melek Ahmet Paşa Mosque) in the city brought the thought that there was not a qualified and/or satisfactory tile production in Diyarbakır (Öney, 1987; Kuban, 1970; Dasdağ, 2013). Further-more, both the body and slip layer possessed a very clean white view, and the colors were extremely vivid with the excellent tones for the Iznik tiles (until the early 17th century AD), whereas the body was yellow-ish, the slip layer was off-white and the colors were distorted (particularly the pale red ones) for Diyarba-kır tiles (Yıldırım, 2005). Considering such infor-mation together with the buff, pink and cream colors of the bodies (Table 2), the tiles in the present study seem to belong to a local production using regional raw material comprising carbonates (CaO content; 7.52-22.77 wt.% identified by EDX) which is abundant in the region (i.e. marble, limestone) (MTA 2019a, 2019b, 2019c). The application of a lead-alkali glaze on a calcareous clay body looks reasonable, since there is a less possibility of glaze defects in comparison with a non-calcareous clay body as the expansion coeffi-cient of the calcareous clay bodies (in the range of 0-500°C) are, in general, consistent with that of the lead-alkali glazes (Tite et al., 1998).

3.2. Characterization of ceramic bodies

3.2.1. Chemical composition

The amounts (wt.%) of SiO_2 (58.08), Al_2O_3 (8.92), CaO (10.92), Na_2O (2.15), K_2O (3.06) and MgO (6.76) detected by EDX for the tile body of PS-1 suggested use of calcareous raw materials in production of the main texture of the tile, particularly considering the amount of CaO (Maniatis et al., 1981). Thanks to the presence of FeO (7.57 wt.%), the pinkish cream color of the body (Table 2) is thought to be brought by iron minerals, particularly with hematite which gives such colors in oxidizing firing environment (Issi et al., 2011). In p-XRF analysis of the paste, the absence and/or ignorable amounts of Cu, Sn and Pb pointed

out that such elements would have originated from the glaze.

The detected amounts (wt.%) of SiO_2 (71.21), Al_2O_3 (6.93), CaO (7.62), Na_2O (2.39), K_2O (2.86) and MgO (3.24) by EDX for the tile body of PS-2 (Table 3) suggested that the raw material presumably comprised a certain amount of calcareous clay batch (Maniatis et al., 1981) and was rich in quartz (considering relatively the high amount of SiO_2).

EDX results obtained for the tile body of PS-3 (SiO_2:59.96 %, Al_2O_3:4.64 %, CaO:13.20 %, MgO:5.93 %, Na_2O:2.00%, K_2O:1.97 % and FeO 3.69 %) pointed out that the raw material of this tile would be calcareous, mainly due to high CaO (Maniatis et al., 1981).

EDX analysis revealed the presence of SiO_2 (48.76 wt.%), Al_2O_3 (2.42 wt.%), CaO (27.77 wt.%), MgO (3.42 wt.%), Na_2O (3.66 wt.%), K_2O (1.95 wt.%) and FeO (2.44 wt.%) for the body of PS-4. The high amount of CaO, in particular, suggested use of calcareous clay batch for the body (Maniatis et al., 1981). The excessive amount of CaO (27.77 wt.%) was also attributed to the presence of plaster formerly used on the interior walls of the mosque, particularly with the purpose of imitating the original tiles by oil paint (Table 1). The plaster residues might have penetrated towards the porous tile body, and it would have not been totally removed in the course of purification process of the tiles before the analyses. CuO was also detected by EDX in the body composition. Considering the initial application of the liquid glaze on the surface, this case is assigned to the fact that the glaze

components could have been occasionally absorbed by the tile body (depending on the grain size, coefficients of thermal expansion, porosity, application conditions of the glaze on the tile surface etc., as well).

The body of PS-5 was found to possess mainly SiO_2 (62.26 wt.%), Al_2O_3 (8.23 wt.%), CaO (8.83 wt.%), MgO (6.81 wt.%), Na_2O (3.96 wt.%), K_2O (2.27 wt.%) and FeO (5.01 wt.%). This data, mainly the amount of CaO, indicated to carbonates in the raw material (Maniatis et al., 1981). Considering the amount of CaO (7.14 wt.%) identified in body composition of PS-6 through EDX, it was deduced that calcareous minerals (in certain rates) could take place in the raw material (Maniatis et al., 1981).

The presence of SO_3 (Table 3), which was occasionally detected for the samples' bodies in various amounts (1.38 wt.% in PS-1, 2.35 wt.% in PS-2, 8.13 wt.% in PS-3, 6.45 wt.% in PS-4, 0.84 wt.% in PS-5, 1.60 wt.% in PS-6) indicated that the deteriorations on the walls, and therefore on the tiles, might have occurred mostly due to the salts comprising sulphate compounds. The scatter plots derived from Al_2O_3 vs. SiO_2 amounts and Al_2O_3/SiO_2 vs. CaO/SiO_2 ratios (using EDX data of the tile bodies) showed that PS-4 (monochrome) and PS-6 (polychrome) distinctively, and PS-2 (polychrome) slightly differ from the others (Fig. 8). This relation between the main oxides (Al_2O_3 and SiO_2) in ceramic paste may suggest use of different clay batches in production of such tile bodies.
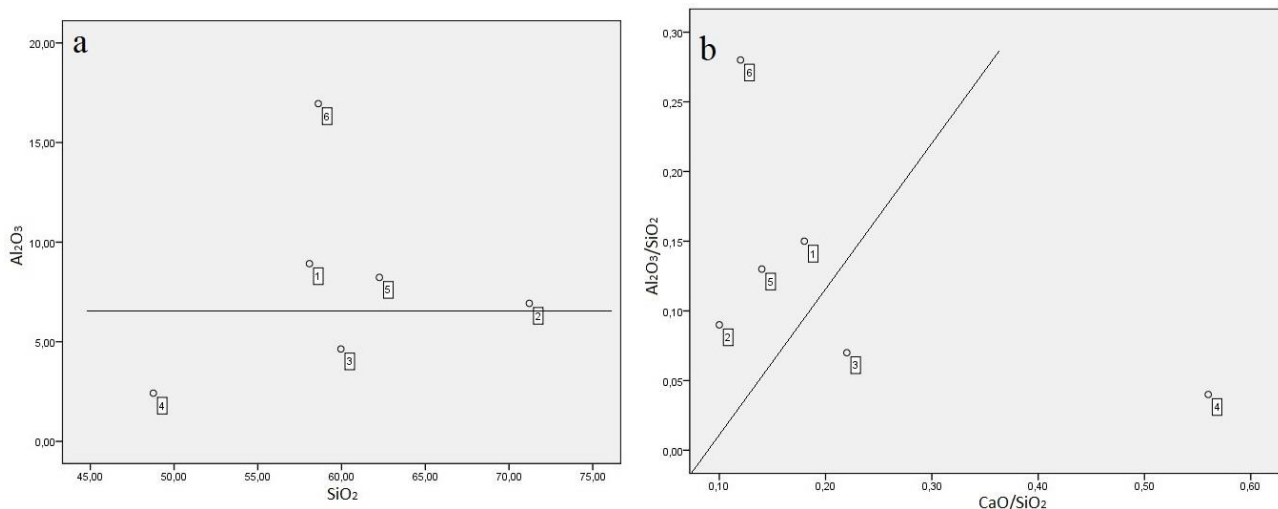

Figure 8. Scatter plots of (a) Al2O3 vs. SiO2 and (b) Al2O3/SiO2 vs. CaO/SiO2 ratios identified by EDX (wt.%) for bodies. The numbers represent to the sample code (e.g. 1: PS-1). (Lines are subsequently drawn as a guide for assessing the results.)

3.2.2. XRD and petrography

The bodies of the glazed tiles were exposed to various analytical techniques, which are frequently preferred in ceramic archaeometry (Bayazit et al., 2014; Bayazit 2018; Germinario et al., 2019; Kałużna-

Czaplińska et al., 2017; Drebushchak et al., 2018; Medeghini et al., 2019) in order to find out the mineralogical content and enlighten the diagnosis of the paste. XRD, petrography, FTIR and TG-DTA pro-

vided a directive knowledge regarding the mineralogical composition of the tiles which gave the opportunity to elucidate the production technology of the tiles.

According to petrography and XRD results quartz, plagioclase and opaque minerals (e.g. hematite, magnetite) were determined in all of the tiles, while chert and quartzite were found as the rock contents (Table 6). Biotite, sericite, granite, and grog were occasionally identified for the samples. It was found by the petrographic examination that the tiles consisted of coarse and particularly the medium sized aggregates (originated from igneous rocks) which seemed to happen likely due to the high amounts of non-plastic inclusions (e.g. quartz). Total aggregate proportion through the paste was found to change in the range of 75-82 vol. %. Being parallel to this, the relatively high non-plastic material/matrix ratio could also be observed on microphotographs of the tile bodies (Fig. 9). The presence of grog was assigned to use of temper material that would be added to control the physical features of the body during the drying and firing process (Rice, 1987). Considering the presence of quartz, chert (Fig. 9-e) and quartzite, it was thought that the temper material would be also quartz besides the grog residues (Fig. 9-l) which could have been subsequently added to the raw material.

Table 6. XRD and petrography results of the tile bodies.

Sample	P*	TA*	Mineral/rock*	Mineral**
PS-1	12	75	Q, Ch, Pl, Qs, Op	Q (d), F/Pl, Pr (l)
PS-2	7	80	Q, Ch, Pl, Bi, Op, Sr, Qs, G	Q (d), F/Pl, Pr (l)
PS-3	7	80	Q, Ch, Pl, Bi, Op, Sr, Qs, G	Q (d), F/Pl (l), Pr (l)
PS-4	9	82	Q, Ch, Pl, Bi, Op, G, Qs, Grog	Q (d), F/Pl (sc), Pr (l)
PS-5	7	80	Q, Ch, Pl, Bi, Op, Sr, Qs, G	Q (d), F/Pl (sc), Pr (sc)
PS-6	9	82	Q, Ch, Pl, Bi, Op, G, Qs, Grog	Q (d), F/Pl (l), Pr (sc)

Identified by petrography* and by XRD**. P: porosity (vol. %), TA: total aggregate (vol. %), (d): dominant, (l): low intensity, (sc): scarce. Bi: biotite, Ch: chert, F: feldspar, G: granite, Op: Opaque minerals (e.g. hematite, magnetite), Pl: plagioclase, Pr: pyroxene, Sr: sericite, Q: Quartz, Qs: quartzite.

Quartz was found as the dominant mineral, while pyroxene showed low X-ray intensities on XRD patterns (i.e. PS-1, PS-2, PS-3, PS-4) and was slightly observed for some of the samples (PS-5, PS-6) indicating scarce amounts (Fig. 10). Clay minerals, which would disappear through a decomposition reaction at about 900°C after the dehydroxylation phenomenon around 700-750°C (Cultrone et al., 2001), and carbonates (i.e. calcite, dolomite) were not observed on XRD patterns. For the calcareous ceramics, as in the present study, carbonates begin to decompose around 700-800°C and new phases (i.e. gehlenite, anorthite, pyroxene) occur as the temperature increases (≥800°C) (Cultrone et al., 2001; Fabbri et al., 2014). Decomposition of the minerals and formation of new phases would allow to estimate the firing temperature ranges of ceramics (Cultrone et al., 2001). Thus, considering such reactions, the firing temperature of the tile bodies was predicted as ca. 850-900°C mainly due to the absence of carbonates/clay minerals, and presence of poorly formed pyroxene (Grifa et al., 2019).

3.2.3. FTIR and TG-DTA

FTIR test was employed for the powder samples of the tile bodies in order to make a contribution to mineralogical characterization. Representative FTIR spectra are given in Fig. 11 and the whole bands detected in Table 7. The wavenumbers on FTIR spectra were evaluated through the band values in the available literature (Fabbri et al.,2014; Maravelaki-Kalaitzaki and Kallithrakas-Kontos, 2003; Mazzocchin et al., 2003; Edreira et al., 2001; Böttcher et al., 1997; Kurap et al., 2010; De Benedetto et al., 2002; Barone et al., 2011; Ravisankar et al., 2011; Farmer, 1974);

Quartz was identified with the band values of 1163 cm^{-1}, 792-796 cm^{-1}, 773-778 cm^{-1}, 691-693 cm^{-1}, 519 cm^{-1} and 510 cm^{-1}. The wavenumbers of 543 cm^{-1}, 582-589 cm^{-1}, 651 cm^{-1} and 604-607 cm^{-1} were attributed to feldspar/plagioclase. It was predicted that the bands at 1047-1055 cm^{-1}, 971 cm^{-1}, 972 cm^{-1}, 874-879 cm^{-1}, 673-678 cm^{-1}, 635-637 cm^{-1}, 506-513 cm^{-1}, 519 cm^{-1} and 526-530 cm^{-1} were due to pyroxene minerals (i.e. diopsite, augite). While the wavenumbers 534 cm^{-1}, 535 cm^{-1}, 543 cm^{-1}, 551-555 cm^{-1}, 572 cm^{-1} and 651 cm^{-1} were assigned to hematite, 564 cm^{-1} and 575-578 cm^{-1} were thought to point out both hematite and magnetite. The red, brown and/or pink colors of the bodies have strengthened the possibility that these bands belong to hematite which would give such colors in an oxidizing firing.
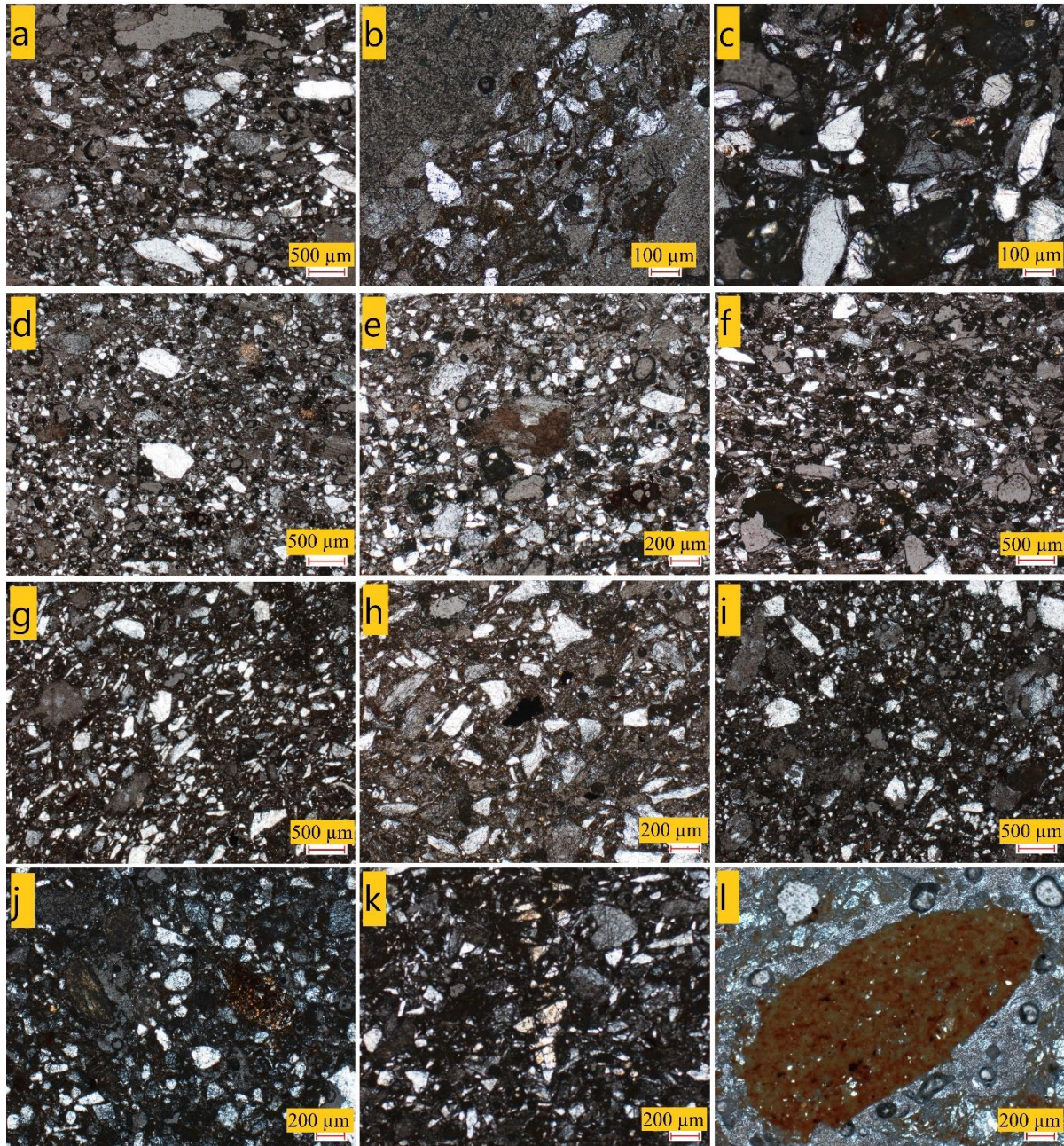
Figure 9. Microphotographs of tile bodies (a) PS-1; general matrix, (b) PS-1; plagioclase, (c) PS-1; pyroxene, (d) PS-2; general scan on matrix, (e) PS-2; chert, (f) PS-3; general matrix, (g) PS-4; general matrix, (h) PS-4; opaque mineral (e.g. hematite, magnetite), (i) PS-5; general matrix, (j) PS-5; pyroxene, biotite, (k) PS-6; general matrix, (l) PS-6; grog (tile/brick fragment).
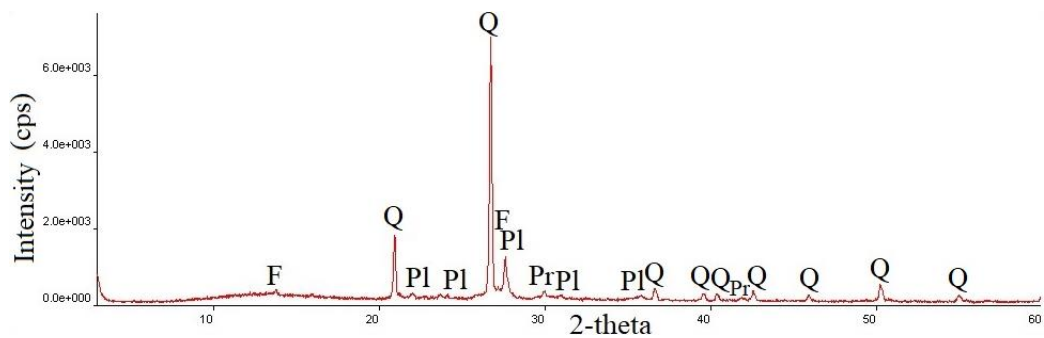

Figure 10. Typical XRD pattern of the sample PS-2 (F: feldspar, Pl: plagioclase, Pr: pyroxene, Q: quartz).

In a comprehensive study of De Bonis et al. (2017) concerning on formation of different shades of red in Ca-rich and Ca-poor ceramics (respectively from the Island of Ischia and Sorrento Peninsula), the results suggested that the red hues in Ca-poor samples are relatively more intense at higher temperatures at which the hematite amounts increased, whereas the red hue in Ca-rich samples was seen to increase till about 900°C and color saturation was reduced as the neo-formations (i.e. pyroxene, melilite), which were thought to avoid the generation of hematite, occurred (De Bonis et al., 2017). In the present work, the firing temperature of the tile bodies (ca. 850-900°C) and presence of pyroxene suggested that the formation of hematite in the ceramic matrix, and therefore its color saturation, could be hindered due to the appearance of neo-formation (pyroxene), and the light red/buff colors of the bodies could be likely due to low amounts of hematite and/or fine grains of iron (De Bonis et al., 2017).
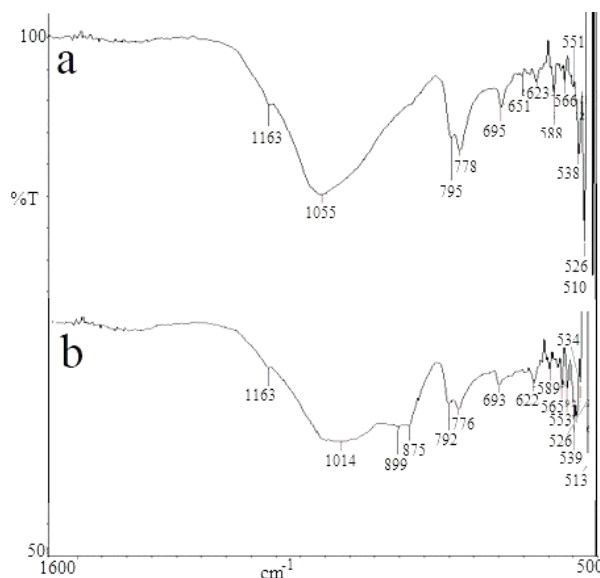
Figure 11. Typical FTIR spectrum of the sample (a) PS-2 and (b) PS-5.

Table 7. Wavenumbers detected for the tile bodies by FTIR.

Sample	Wavenumber (cm^{-1})
PS-1	972/879/618/582/572/563/555/535/530/506
PS-2	1163/1055/795/778/695/651/623/588/566/551/538/526/510
PS-3	1047/971/864/796/774/693/673/635/619/604/588/576/564/551/543/530
PS-4	1048/898/794/777/693/678/623/605/588/578/554/539/527/463
PS-5	1163/1014/899/875/792/776/693/622/589/565/553/539/534/526/513
PS-6	1003/773/727/691/637/619/607/589/575/563/554/530/528/519

Finally, some of the wavenumbers were not certainly assigned to one-only mineral, because there would be overlapping among the band values. For instance, 463 cm^{-1}, 1003 cm^{-1}, 1014 cm^{-1}, 1047 cm^{-1}, 1048 cm^{-1}, 1055 cm^{-1} mainly indicated to the presence of feldspar/plagioclase, but they were also close to the wavelength numbers of clay minerals and high temperature minerals which include Al and Si, likewise the feldspars/plagioclases. Additionally, the band values of 563-566 cm^{-1} indicated to iron minerals, but as the crystallization of calcium silicates at high temperatures ($\geq$ 800-900°C) would be seen in the same range, those bands could also represent neo-formations. Hereby, indication of other prospective minerals through the same or close band values should be additionally considered (Issi et al., 2011; Fabbri et al., 2014; Grifa et al., 2019; Edreira et al., 2001; De Benedetto et al., 2002; Barone et al., 2011; Ravisankar et al., 2011; Farmer 1974).

TG-DTA was additionally performed on powder samples of the tile bodies in order to examine the thermal characteristics of the raw materials. The results obtained through TG-DTA technique were evaluated as follows (Fabbri et al.,2014; Palanivel and Kumar 2011; Meyvel et al.,2012; Maritan et al., 2006);

• The endothermic effect on DTA curves in the range of 25-200°C, which indicates the presence of hygroscopic water, was negligible in two samples (PS-1 and PS-6) and relatively obvious in one sample (PS-3), but no such effect was observed for the other samples.

- On DTA curves, the exothermic effect in the range of 200-600°C, indicating the presence of organic matter, was observed only for one sample (PS-3).
- No endothermic effect in the range of 600-850°C indicating the presence of carbonates (calcite, dolomite, etc.) was found in any sample. This result indicated that the carbonates had decomposed. The negligible weight loss values at 600-850°C also confirmed the prediction (Table 8).

- The absence of evident enthalpy changes on the DTA curves and the negligible weight losses (0.216-0.963 wt.%) above 950°C indicated that the maximum firing temperatures of the tiles were not higher than 950-1000°C.

It was observed that the data obtained by both FTIR and DTA well matched with the petrography and XRD results. The firing temperature of the tile bodies are approved by the IR bands and enthalpy changes together with the weight loss values.

Table 8. Weight loss values observed at specific temperature ranges.

	Initial weight	Temperature range (°C)					Total weight loss	Residual mass
		25-200	200-400	400-600	600-850	850-1000		
Sample	mg	wt.%					mg	mg
PS-1	7,473	-0,308	-0,549	-0,415	-0,455	-0,308	0,152	7,321
PS-2	7,687	-0,299	-0,559	-0,689	-0,963	-0,130	0,203	7,484
PS-3	7,872	-1,118	-1,435	-0,635	-0,216	-0,749	0,327	7,545
PS-4	7,955	-0,302	-0,867	-0,603	-0,541	-0,126	0,194	7,761
PS-5	7,820	-0,307	-0,729	-0,627	-0,716	-0205	0,202	7,618
PS-6	6,579	-0,699	-0,562	-0,714	-0,623	-0,182	0,183	6,396

4. CONCLUSION

Six characteristic glazed tiles, which were selected to represent the whole tile repertoire of Parlı Safa Mosque of Diyarbakır, were investigated in an archaeometric way using multiple analysis methods. According to the results, the relatively high amount of CaO content (7.52-22.77 wt.%) in tile bodies indicated that the raw materials would have comprise carbonates. The excess amount of CaO detected for the body of sample PS-4 (22.77 wt.%) was not totally assigned to the carbonates from the raw material, it was also attributed to the presence of plaster (calcium sulphate) which was utilized as a base under the oil painting employed for imitating the ornamentations on the tiles (seems like a tentative solution, in a way).

The occasional existence of SO_3 in tile bodies likewise could be due to plaster. Yet, Ca-sulphate compounds were not detected by mineralogical analyses, but this would have been due to their trace or scarce amounts (if the assumption was right; use of plaster as a base under the oil painting). Although the purification/cleaning process has been performed with precision, the porous structure of the body could allow such impurities to diffuse into the structure. For the body of the tiles, it was observed that the firing temperature was about 850-900°C due to the presence of pyroxene (low/scarce), and absence of carbonates and clay minerals. The temperature was also proved by FTIR, which showed the bands suggesting the existence of pyroxene and crystallization of calcium sil-

icates, and by TG-DTA in which there was no endothermic effect at 600-850°C and no clear enthalpy changes above 950°C.

The colored glazes were thoroughly investigated by EDX, and p-XRF was employed as a complementary technique which provided significant information about the chemical composition of the glazes. It was deduced from the results that the blue turquoise and light blue were obtained by copper in the glazes which possess high alkali content and low amount of lead (i.e. PS-1, PS-3, PS-4 and PS-5). Dark blue was found to be achieved mainly by cobalt (i.e. PS-2, PS-3 and PS-6). The whole results suggested that while the alkaline oxides in the glazes brought the blue colorings, increase in lead amount provided the green color on the same surface of the tile (i.e. PS-3). Being identified on the glaze layers of PS-1 and PS-6, tin was considered as a complementary element taking place in the occurrence of the blue colors, and also as an opacifier for the glazes. Considering their chemical compositions, the black contours were thought to be achieved by using different combinations of Fe, Mn and Cr. Manganese was also found to be effective in emergence of dark brown. As far as the formation of the colors is concerned, the firing atmosphere (i.e. reducing, oxidizing or neutral) during the heating and cooling process should be also taken into account.

The body and colored glazes of the tiles to be produced in restoration applications in accordance with the data presented in this study could be beneficial for preserving the original properties of the building and transferring it to future generations. As in the case

discussed in this research, the obtained data from archaeometry studies should be considered before restoration implementations. In this context, archaeometry is an interdisciplinary science to serve for restoration and conservation process in terms of both documentation and providing data.

ACKNOWLEDGEMENTS

REFERENCES

Archives of General Directorate of Foundations (VGM). (2019) Turkey.

Belfiore, C. M., Mazzoleni P., Manenti, A.M., Mastelloni, M. A., Corsale, V., Barone, G. (2021) Non-Destructive XRF analysis of Aegyptiaca from Sicilian Archaeological Sites, *Mediterranean Archaeology and Archaeometry*, Vol. 21, No. 1, pp. 37-69. https://doi.org/10.5281/zenodo.4284407

Barone, G., Crupi, V., Longo, F., Majolino, D., Mazzoleni, P., Tanasi, D., Venuti, V. (2011) FT-IR spectroscopic analysis to study the firing process of prehistoric ceramics. *J. Mol. Struct.,* Vol. 993, pp. 147-150.

Baş, G. (2006) Diyarbakır'daki İslam dönemi mimarisinde süsleme (in Turkish), Van Yüzüncü Yıl University, Institute of Social Science, Art History, PhD thesis, Van, Turkey.

Bayazit, M., Işık, I., Issi, A., Genc, E. (2014) Spectroscopic and thermal techniques for the characterization of the first millennium AD potteries from Kuriki-Turkey. *Ceram. Int.,* Vol. 40, pp. 14769-14779.

Bayazit, M. (2018) Archaeometric study of possible Ninevite-5 pottery from upper Tigris region using SEM-EDS, PEDXRF, and OM. *X-Ray Spectrom.*, Vol. 47, pp. 92-104.

Beysanoğlu, Ş. (1996) Anıtları ve kitabeleri ile Diyarbakır tarihi (in Turkish), Cilt:1, Ankara.

Bianchin, S., Favaro, M., Vigato, P.A., Botticelli, G., Germani, G., Botticelli, S. (2009) The scientific approach to the restoration and monitoring of mural paintings at S. Girolamo Chapel – SS. Annunziata Church in Florence. *J. Cult. Herit.,* Vol. 10, No. 3, pp. 379-387.

Böttcher, M. E., Gehlken, P. L., Steele, D. F. (1997) Characterization of inorganic and biogenic magnesian calcites by Fourier Transform infrared spectroscopy. *Solid State Ionics.,* Vol. 101-103, pp. 1379-1385.

Caggiani, M. C., Colomban, Ph., Valotteau, C., Mangone, A., Cambon, P. (2013) Mobile Raman spectroscopy analysis of ancient enamelled glass masterpieces. *Anal. Methods.*, Vol. 5/17, pp. 4345-4354.

Colomban, Ph. (2003) Lapis lazuli as unexpected blue pigment in Iranian Lâjvardin ceramics. *J. Raman Spectrosc.*, Vol. 34 No. 6, pp. 420–423.

Colomban, Ph., Milande, V., Le Bihan, L. (2004) On-site Raman analysis of Iznik pottery glazes and pigments. *J. Raman Spectrosc.*, Vol. 35, No. 7, pp. 527-535.

Constantinescu, B., Cristea-Stan, D., Kovàcs, I., Szökefalvi-Nagy, Z. (2014) External milli-beam PIXE analysis of the mineral pigments of glazed Iznik (Turkey) ceramics. *Period. Mineral.,* Vol. 83, No. 2, pp. 159-169.

Cultrone, G., Rodriguez-Navarro, C., Sebastian, E., Cazalla, O., De La Torre, M.J. (2001) Carbonate and silicate phase reactions during ceramic firing. *Eur. J. Mineral.,* Vol. 13, pp. 621-634.

Dabanlı, Ö., İş, M., Özbaş, F., Yaşayan. G. (2018) Diyarbakır Parlı Sefa Camii çini analiz projesi raporu (in Turkish). FSMVU Research Center for Conservation of Cultural Heritage (KURAM).

Dasdağ, F. E. (2013) Melek Ahmet Pasha Mosque tiles of Diyarbakır. *Electronic Journal of Social Sciences.*, Vol. 12, No. 45, pp. 270-280.

De Benedetto, G. E., Laviano, R., Sabbatini, L., Zambonin, P. G. (2002) Infrared spectroscopy in the mineralogical characterization of ancient pottery. *J. Cult. Herit.*, Vol. 3, No. 3, pp. 177-186.

De Bonis, A., Cultrone, G., Grifa, C., Langella, A., Leone, A.P., Mercurio, M., Morra, V. (2017) Different shades of red: The complexity of mineralogical and physico-chemical factors influencing the colour of ceramics, *Ceram. Int.*, Vol. 43, No. 11, pp. 8065-8074.

Demiriz, Y. (2002) Osmanlı çini sanatı (in Turkish), Türkler, Cilt 12, Ankara, pp. 563-572.

Drebushchak, V. A., Mylnikova, L. N., Drebushchak, T. N. (2018) Thermoanalytical investigations of ancient ceramics. *J. Therm. Anal. Calorim.*, Vol. 133, No. 1, pp. 135-176.

Ebaid, S., and Ghaly, N. (2013) Ceramic mihrabs in religious buildings in Bukhara during 16th C. *Mediterranean Archaeology and Archaeometry*, Vol. 13, No. 2, pp. 43-56.

Edreira, M. C., Feliu, M. J., Fernández-Lorenzo, C., Martin, J. (2001) Roman wall paintings characterization from Cripta del Museo and Alcazaba in Mérida (Spain): chromatic, energy dispersive X-ray flurescence spectroscopic, X-ray diffraction and Fourier transform infrared spectroscopic analysis. *Anal. Chim. Acta.*, Vol. 434, pp. 331-345.

Fabbri, B., Gualtieri, S., Shoval, S. (2014) The presence of calcite in archeological ceramics. *J. Eur. Ceram. Soc.*, Vol. 34, No. 7, pp. 1899-1911.

Farmer, V.C. (1974) Infrared Spectra of Minerals. London: Mineralogical Society of Great Britain and Ireland.

Fischer, C., Hsieh., E. (2017) Export Chinese blue-and-white porcelain: compositional analysis and sourcing using non-invasive portable XRF and reflectance spectroscopy. *J. Archaeol. Sci.*, Vol. 80, pp. 14-26.

Germinario, C., Cultrone, G., Cavassa, L., De Bonis, A., Izzo, F., Langella, A., Mercurio, M., Morra, V., Munzi, P., Grifa, C. (2019) Local production and imitations of Late Roman pottery from a well in the Roman necropolis of Cuma in Naples, Italy. *Geoarchaeology,* Vol. 34, pp. 62-79.

Grifa, C., Germinario, C., De Bonis, A., Langella, A., Mercurio, M., Izzo, F., Smiljanic, D., Guarino, V., Di Mauro, S., Soricelli, G. (2019) Comparing ceramic technologies: The production of Terra Sigillata in Puteoli and in the Bay of Naples. *J. Archaeol. Sci. Reports,* Vol. 23, pp. 291-303.

Gürsoy, S. (1993) Diyarbakır eski mimarisinde çini süslemesi (in Turkish), Dicle University, Institute of Science, Master Thesis, Diyarbakır, Turkey.

Hurst, D., Freestone, I. (1996) Lead glazing technique from a medieval kiln site at Hanley Swan, Worcestershire. *Medieval Ceramics,* Vol. 20, pp. 13-18.

Issi, A., Raškovska, A., Kara, A., Grupce, O., Minčeva-Šukarova, B., Okyar, F. (2011) Scanning electron microscopy and micro-Raman spectroscopy of slip layers of Hellenistic ceramic wares from Dorylaion/Turkey. *Ceram. Int.,* Vol. 37, pp. 1879-1887.

Kałużna-Czaplińska, J., Rosiak, A., Grams, J., Chałupka, K., Makarowicz, P., Maniukiewicz, W., Szubiakiewicz, E. (2017) The Studies of archaeological pottery with the use of selected analytical techniques. Crit. Rev. *Anal. Chem.,* Vol. 47, No. 6, pp. 490-498.

Kuban, D. (1970) 100 soruda Türk Sanat Tarihi (in Turkish), Istanbul.

Kurap, G., Akyuz, S., Akyuz, T., Basaran, S., Cakan, B. (2010) FT-IR spectroscopic study of terra-cotta sarcophagi recently excavated in Ainos (Enez) Turkey. *J. Mol. Struct.*, Vol. 976, No. 1-3. pp. 161-167.

Kühn, H. (1968) Lead-tin yellow, *Stud. Conserv.*, Vol. 13, pp. 7-33.

Liritzis, I., Laskaris, N., Vafiadou, A., Karapanagiotis, I., Volonakis, P., Papageorgopoulou, C., Bratitsi, M. (2020) Archaeometry: an overview scientific culture, *Scientific Culture,* Vol. 6, No. 1, pp. 49-98. https://doi.org/10.5281/zenodo.3625220

Maniatis, Y., Simopoulos, A., Kostikas, A. (1981) Moessbauer study of the effect of calcium content on iron oxide transformations in fired clays. *J. Am. Ceram Soc.*, Vol. 64, No. 5, pp. 263-269.

Maravelaki-Kalaitzaki, P., Kallithrakas-Kontos, N. (2003) Pigment and terracotta analyses of Hellenistic figurines in Crete. *Anal. Chim. Acta.*, Vol. 497, pp. 209-225.

Maritan, L., Nodari, L., Mazzoli, C., Milano, A., Russo, U. (2006) Influence of firing conditions on ceramic products: Experimental study on clay rich in organic matter. *Appl. Clay Sci.*, Vol. 31, pp. 1-15.

Mason, R. B., Tite., M. S. (1997) The beginnings of tin-opacification of pottery glazes. *Archaeometry,* Vol. 39, pp. 41-58.

Mazzocchin, G.A., Agnoli, F., Colpo, I. (2003) Investigation of Roman Age pigments found on pottery fragments. *Anal. Chim. Acta.*, Vol. 478, pp. 147-161.

Medeghini, L., Fabrizi, L., De Vito, C., Mignardi, S., Nigro, L., Gallo, E., Fiaccavento, C. (2016) The ceramic of the "Palace of the Copper Axes" (Khirbet al-Batrawy, Jordan): A palatial special production. *Ceram. Int.*, Vol. 42, No. 5, pp. 5952-5962.

Medeghini, L., Sala, M., De Vito, C., Mignardi, S. (2019) A forgotten centre of ceramic production in Southern Levant: Preliminary analytical study of the Early Bronze Age pottery from Tell el-Far'ah North (West Bank). *Ceram. Int.,* Vol. 45, No. 9, pp. 11457-11467.

Messina M., Arcifa, L., Barone G., Finocchiaro, C., Mazzoleni, P. (2018) Islamic pottery production in eastern Sicily (10th-11th centuries): preliminary archaeometric data on local and imported products from paternò (Sicily). *Mediterranean Archaeology and Archaeometry*, Vol. 18, No. 5, pp. 207-223. https://doi.org/10.5281/zenodo.1285914

Meyvel, S., Sathya, P., Velraj, G. (2012) Thermal characterization of archaeological pot sherds recently excavated in Nedunkur, Tamilnadu, India. *Cerâmica,* Vol. 58, pp. 338-341.

MTA (2019a) MTA Turkey official website. Accessed November 20, 2019. http://www.mta.gov.tr/v3.0/sayfalar/hizmetler/maden-haritalari/diyarbakir.pdf

MTA (2019b) MTA Turkey official website. Accessed November 20, 2019. http://www.mta.gov.tr/v3.0/sayfalar/hizmetler/maden-haritalari/batman.pdf

MTA (2019c) MTA Turkey official website. Accessed November 20, 2019. http://www.mta.gov.tr/v3.0/sayfalar/hizmetler/maden-haritalari/mardin.pdf

Öney, G. (1987) Ceramic Tiles in Islamic Architecture, Ada Press Publishers, Istanbul.

Palanivel, R., Rajesh Kumar, U. (2011) Thermal and spectroscopic analysis of ancient potteries. Rom. *J. Phys.*, Vol. 56, pp. 195-208.

Ravisankar, R., Kiruba, S., Naseerutheen, A., Chandrasekaran, A., Annamalai, G.R., Seran, M., Balaji, P.D. (2011) Estimation of the firing temperature of archaeological pottery excavated from Thiruverkadu, Tamilnadu, India by FT-IR spectroscopy. *Archives of Physics Research,* Vol. 2 No. 4, pp. 108-114.

Rice, P. M. (1987) Pottery analysis: A sourcebook, Chicago: University of Chicago Press.

Panagopoulou, A., Lampakis, D., Christophilos, D., Beltsios, K., Ganetsos, Th. (2018) Technological examination of Iznik ceramics by SEM-EDX, RAMAN, XRD, PLM: A case study. *Scientific Culture*, Vol. 4, No. 3, pp. 27-33. https://doi.org/10.5281/zenodo.1409802

Simsek, G., Unsalan, O., Bayraktar, K., Colomban, P. (2019a) On-site pXRF analysis of glaze composition and colouring agents of "Iznik" tiles at Edirne mosques (15th and 16th-centuries). *Ceram. Int.*, Vol. 45, No. 1, pp. 595-605.

Simsek, G., Demirsar Arli, B., Kaya, S., Colomban., P. (2019b) On-site pXRF analysis of body, glaze and colouring agents of the tiles at the excavation site of Iznik kilns. *J. Eur. Ceram. Soc.*, Vol. 39, No. 6, pp. 2199-2209.

Sözen, M. (1971) Diyarbakır'da Türk mimarisi (in Turkish), Diyarbakır'ı Tanıtım ve Turizm Derneği Yayınları, İstanbul.

Tite, M. S., Freestone, I., Mason, R., Molera, J., Vendrell-Saz, M., Wood, N. (1998) Lead glazes in antiquity-methods of production and reasons for use. *Archaeometry,* Vol.40, No. 2, pp. 241-260.

Tite, M., Pradell, T., Shortland, A. (2008) Discovery, production and use of tin-based opacifiers in glasses, enamels and glazes from the late Iron Age onwards: a reassessment, *Archaeometry*, Vol. 50, pp. 67-84.

Tuncer, O. C. (1996) Diyarbakır Camileri (in Turkish), Diyarbakır Büyük Şehir Belediyesi Kültür ve Sanat Yayınları, Ankara.

Uzun, Z., Köse, C., Köse, N. (2018) A multidisciplinary study to reveal the historical value of wooden structures and to develop a conservation approach: Dere and Karlı Mosques in Samsun, Turkey. *J. Cult. Herit.*, Vol. 32, pp. 60-72.

Wood, N., Henderson, J., Tregear, M. (1989) An examination of Chinese fahua glazes, in: J. Li, X. Chen (Eds.), Proceedings of the 1989 International Symposium on Ancient Ceramics, Shanghai Res. Soc. Sci. Technol. Ancient Ceram., Shanghai, pp. 172-82.

Yastı, Ş. Y. (2011) Konya Kubad Abad çinilerinin arkeometrik karakterizasyonu ve benzeri çinilerin araştırması (in Turkish), Selçuk University, Institute of Science, Department of Mining Engineering, PhD Dissertation, Konya.

Yediyıldız, B. (2008) Osmanlı öncesi Diyarbakır'ına genel bir bakış (in Turkish), in: B. Yediyıldız and K. Tomenendal (Eds.), Osmanlı'dan Cumhuriyet'e Diyarbakır, Diyarbakır Valiliği ve Türk Kültürünü Araştırma Enstitüsü Yayını, Ankara, pp. 17-38.

Yıldırım, S. (2001) Diyarbakır yapılarında çini süsleme (in Turkish), Ankara University, Institute of Social Science, Master Thesis, Ankara, Turkey.

Yıldırım, S. (2005). Diyarbakır yapılarındaki Osmanlı dönemi çinilerinin tarihlendirmeleri ve üretim yeri hakkında düşünceler. *Erdem,* Vol. 15, No. 43, pp. 119-144.

Zacharias, N., Palamara E., Kordali R., Muros V. (2020) Archaeological glass corrosion studies: composition, environment and content. *Scientific Culture*, Vol. 6, No. 3, pp. 53-67. https://doi.org/10.5281/zenodo.4007562